Theoretical physics

Original article
UDC 538.911; 539.1.03
DOI: https://doi.org/10.18721/JPM.14414

CHANNELING AND RADIATION OF ELECTRONS AND POSITRONS IN THE DIAMOND HETEROCRYSTALS

A. V. Pavlov [1], A. V. Korol [2], V. K. Ivanov [1]✉, A. V. Solov'yov [2]

[1] Peter the Great St. Petersburg Polytechnic University, St. Petersburg, Russia;

[2] MBN Research Center UG, Frankfurt am Main, Germany

✉ ivanov@physics.spbstu.ru

Abstract: We analyze numerically the radiative and channeling properties of ultra-relativistic electrons and positrons propagating through a periodically bent diamond crystal grown on a straight single-crystal diamond substrate. Such systems are called heterocrystals being one of the experimentally realized specimens for the implementation of crystalline undulators. We state that in such systems the channeling and radiative properties of projectiles are sensitive to the projectiles' energy and to the beam propagation direction, e. g., to the beam-to-crystal site of entry: from the side of substrate or from that of periodically bent crystal. The results obtained are important for designing and practicing the new crystalline undulators.

Keywords: periodically bent diamond crystal, channeling, ultra-relativistic particle, channeling radiation

Funding: The work was supported in part by the DFG (Project No. 413220201) and by the N-LIGHT Project within the H2020-MSCA-RISE-2019 call (GA 872196).

For citation: Pavlov A. V., Korol A. V., Ivanov V. K., Solov'yov A. V., Channeling and radiation of electrons and positrons in the diamond heterocrystals, St. Petersburg Polytechnical State University Journal. Physics and Mathematics. 14 (3) (2021) 190–201. DOI: https://doi.org/10.18721/JPM.14414

Научная статья
УДК 538.911; 539.1.03
DOI: https://doi.org/10.18721/JPM.14414

КАНАЛИРОВАНИЕ И ИЗЛУЧЕНИЕ ЭЛЕКТРОНОВ И ПОЗИТРОНОВ В ГЕТЕРОКРИСТАЛЛАХ АЛМАЗА

А. В. Павлов [1], А. В. Король [2], В. К. Иванов [1]✉, А. В. Соловьев [2]

[1] Санкт-Петербургский политехнический университет Петра Великого, Россия;

[2] Научно-исследовательский центр мезобионаносистем (MBN),
г. Франкфурт-на-Майне, Германия

✉ ivanov@physics.spbstu.ru

Аннотация: В статье проводится численный анализ свойств излучения и каналирования ультрарелятивистских электронов и позитронов, которые распространяются через

периодически изогнутый кристалл алмаза, выращенный на прямой монокристаллической алмазной подложке. Подобные системы называются гетерокристаллами, и они являются одним из экспериментально реализованных образцов на пути создания кристаллических ондуляторов. Утверждается, что в таких системах свойства каналирования и излучения частиц чувствительны к их энергии, а также к направлению распространения пучка, в частности, к месту вхождения пучка частиц в кристалл: со стороны подложки или со стороны периодически изогнутого кристалла. Полученные результаты важны для проектирования, создания и практической реализации новых кристаллических ондуляторов.

Ключевые слова: периодически искривленный кристалл алмаза, каналирование, ультрарелятивистская частица, излучение при каналировании

Финансирование: Работа выполнена при частичной финансовой поддержке гранта Немецкого научно-исследовательского сообщества (DFG, проект № 413220201) и проекта N-LIGHT в рамках междисциплинарного исследовательского сотрудничества H2020-MSCA-RISE-2019 (GA 872196).

Для цитирования: Павлов А. В., Король А. В., Иванов В. К., Соловьев А. В. Каналирование и излучение электронов и позитронов в гетерокристаллах алмаза // Научно-технические ведомости СПбГПУ. Физико-математические науки. 2021. Т. 14. № 4. С. 190–201. DOI: https://doi.org/10.18721/JPM.14414

Introduction

Development of the light sources with photon energy $E >> 10$ keV is an ambitious goal for modern physics. Such sources can be used in various new experimental and technological applications [1 – 5]. One of the systems suitable for this task is a crystalline undulator (CU), which stands for a periodically bent oriented crystal and a beam of ultra-relativistic particles that undergo channeling motion [6]. The periodic bending of the crystal planes gives rise to a strong, undulator-type CU radiation (CUR) in the photon energy between 0.1 and 10 MeV [7 – 9].

Several approaches have been applied to produce periodically bent (PB) crystalline structures. The most studied system is a strained $Si_{1-x}Ge_x$ superlattice in which the concentration x of the dopant atoms is varied periodically [10]. Such crystals, produced at Aarhus University (Denmark) by means of molecular beam epitaxy, have been used in recent channeling experiments with 855 MeV electrons at the MAinzer MIcrotron (MAMI) facility [11, 12] and with 16 GeV electrons at the SLAC facility [13].

Periodic bending can also be achieved by graded doping during synthesis to produce diamond superlattice [14]. Both boron and nitrogen are soluble in diamond, however, higher concentrations of boron can be achieved before extended defects appear [14, 15]. The advantage of a diamond crystal is radiation hardness allowing it to maintain the lattice integrity in the environment of very intensive beams [16].

Boron-doped diamond layer cannot be separated from a straight/unstrained substrate (SC) on which the superlattice is synthesized. Therefore, unlike $Si_{1-x}Ge_x$ superlattice, a diamond-based superlattice has essentially a heterocrystal structure, i.e., it consists of two segments: a straight single-crystal diamond substrate and a PB layer [17].

In this paper, we present results of the computational analysis of channeling and radiative properties of experimentally realized [17] diamond-based CU (Fig. 1). In our simulations, special attention has been paid to the analysis of the new effects which appear due to the presence of the interface between the straight and PB segments in the heterocrystal.

The experiment has been carried out with the 270 – 855 MeV electron beams [11, 18, 19]. For the sake of comparison, the simulations have been carried out for both electron and positron beams. The positron beam of the quoted energy range is available at the DAΦNE acceleration facility [20].

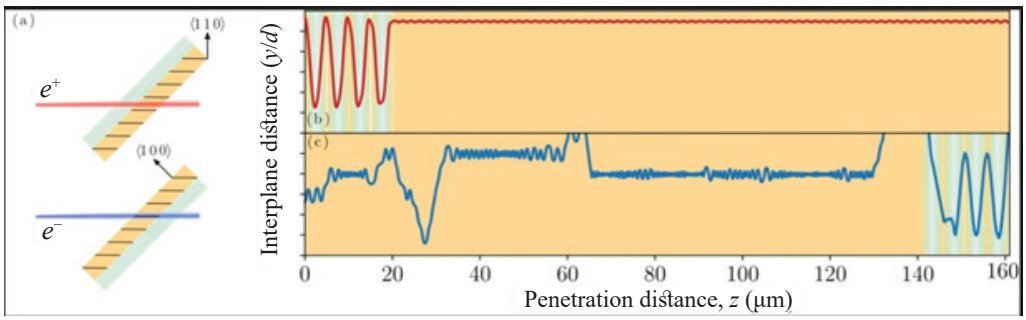

Fig. 1. (*a*): Sketch of the crystal geometry. The diamond single crystal is cut with its surface perpendicular to the [100] direction, then tilted by 45º to orient the (110) planes along the incident beam. The crystal consists of two segments: a straight (S) 141 μm thick single crystal substrate and a boron-doped 20 μm thick periodically bent (PB) segment which accommodates four bending periods [17]. Gradient shading shows the boron concentration which results in the PB of the (110) planes. (*b*) and (*c*): they show two exemplary trajectories of a positron channeled through the whole PB-S crystal (*b*) and an electron in the S-PB crystal (*c*).

Note that several channeling and over-barrier parts the electron's trajectory that are outside the drawing are not shown

Geometry of the system under study is shown in Fig. 1,*a*. The incident beam can enter the crystal at either PB part or a straight (S) one. The crystal must be tilted by 45 º to orient the (110) planes along the incident beam. Hence, there are two possible orientations of the heterocrystal with respect to the incident beams.

To distinguish the crystal orientation with respect to the incident beam, in the text below we refer to the crystal shown at the top of the panel (*a*) as to the PB-S crystal and at the bottom of this panel as to the S-PB crystal (see Fig. 1,*a*). To illustrate the particle's propagation through the crystal, the selected trajectories of a positron (red curve, panel (*b*)) and an electron (blue curve, panel (*c*)) are shown.

The parameters of the heterocrystal used in the simulations of channeling along the (110) plane correspond to those used in the experiment [17]. Namely, total thickness in the beam direction is L_{cr} = 161 μm out of which 141 μm corresponds to the straight segment and 20 μm does to the PB segment.

The bending profile cosine $a\cdot\cos(2\pi z/\lambda_u)$ was assumed with the coordinate z measured along the beam direction. The bending amplitude and period are $a = 2.5$ Å and $\lambda_u = 5$ μm, respectively.

In the straight crystal a particle can experience quasi-periodic channeling oscillations. In addition to these, a channeling particle in the PB segment is involved in the periodic motion due to the periodic bending of a channel. Spectral distribution of the radiation emitted in the heterocrystal bears features of both types of the oscillatory motion. For each trajectory simulated spectral distribution of electromagnetic radiation was calculated within the opening angle $\theta_0 = 0.24$ mrad, which corresponds to one of the detector apertures used at MAMI [11].

Numerical modeling of the channeling and radiation emission processes was performed using MBN Explorer computational software [21]. By means of its channeling module [22] it is possible to simulate the motion of ultra-relativistic particles in different environments, including the crystalline ones. The method of all-atom relativistic molecular dynamics is described in great details in Refs. [22, 23]. This computational package was benchmarked previously for variety of ultra-relativistic projectiles and different crystalline environments [9, 22 – 26].

Using this software in combination with advanced computational facilities it is possible to calculate significant number of projectiles trajectories to analyze. The software also allows one to calculate the radiation distributions $dE/\hbar d\omega$ for each projectile trajectory using the quasi-classical formalism due to V. N. Baier and V. M. Katkov [27]. All this allows one to numerically analyze the channeling, radiation and related phenomena of ultra-relativistic particles in various media, while the accuracy of the predictions made can be compared with that in the experiments.

Results and discussion for positrons

Let us now analyze the case of positron channeling in the heterocrystals. In the planar channeling regime, a charged projectile moves along a crystallographic planes experiencing a collective electrostatic field of the lattice atoms [6]. For positrons, the atomic field is repulsive, so that the particle channels between two adjacent crystalline planes. In this case, nearly harmonic channeling oscillations give rise to narrow photon emission lines.

Fig. 2 presents the spectra calculated for the 270 and 855 MeV projectiles. The spectra consist of two main parts: the CUR (a peak at lower energies) and ChR (a peak at higher ones). The CUR refers to emission from the PB segment while the ChR (Channeling Radiation) can be generated in the PB and the straight segments of the crystal. For the sake of comparison, we quote in Fig. 2 the intensities of the background incoherent bremsstrahlung estimated within the Bethe − Heitler approximation: $2.9 \cdot 10^{-6}$ and $2.5 \cdot 10^{-5}$ for $\varepsilon = 270$ and 855 MeV, respectively.

Fig. 2,*a* shows the results for 270 MeV positrons. The spectra are dominated by the peak of ChR (a strong maximum at $\hbar\omega \approx 0.7$ MeV), CUR reveals itself as a small bump (note the insert in Fig. 2,*a*) in the low energetic region of the spectra $\hbar\omega \approx 0.13$ MeV It is easy to notice that for positrons of 270 MeV the spectral densities of CUR and ChR for PB-S and S-PB crystals are deviate within margin of a statistical error.

The spectra for 855 MeV positrons are shown in Fig. 2,*b*. They consist of two main peaks: the peak of CUR around $\hbar\omega \approx 1.1$ MeV and the one of ChR around $\hbar\omega \approx 3.6$ MeV. One can notice small bumps around $\hbar\omega \approx 2.2$ MeV and $\hbar\omega \approx 7.2$ MeV which aresecond harmonics of CUR and ChR respectively. As well as for 270 MeV positrons intensities of CUR are for two types of crystal, but spectral density of ChR in the S-PB is about 2 times higher than the one in the PB-S. In case of 855 MeV positrons the difference in the intensities between CUR and ChR should be even less pronounced in the experiments, where usually, not the spectral density $dE/\hbar d\omega$ is measured, but the number of photons $(1/\hbar d\omega)\, dE/\hbar d\omega$ with the certain energy.

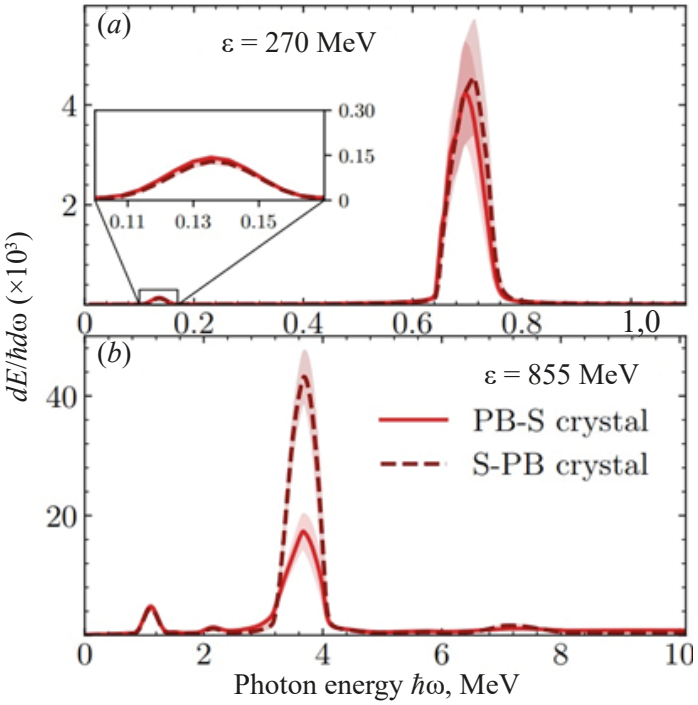

Fig. 2. Radiation spectra produced by 270 (*a*) and 855 MeV (*b*) positrons in the $L_{cr} = 161$ μm diamond (110) PB-S and S-PB crystals (the inset shows 6 times magnified the CUR peak).
The collection angle was set to $\theta_0 = 0.24$ mrad. Shading indicates the statistical error due to the finite number of simulated trajectories

In order to analyze difference in the radiation spectra, let us plot the trajectories of positrons. Fig. 3 presents the exemplary trajectories of the 855 MeV positrons. Fig. 3,*a* shows parts of the trajectories of positrons which channel in the PB-S crystals. In that case positrons firstly enter through the PB crystal and then penetrate through the interface to the SC. For 855 MeV positrons the amplitude of channeling oscillations is strongly suppressed, since the potential barrier is reduced due to centrifugal force [24, 25]. This also results in the strong suppression of ChR for the high energetic particles in the PB diamond crystals. Because of that, the positrons propagating in the PBC, experience strong dechanneling in the parts of the crystal with a large curvature of its planes where the centrifugal force acting on the channeled positron is maximal. However, the opposite process, re-channeling, can occur in the segments of the crystal with a small curvature. Re-channeling causes an effective increase in the total channeling length of the particles. The positrons captured to the channel in the PB segment then penetrate to the straight segment without dechanneling. Propagating through the interface they retain the amplitude of their channeling oscillations.

In opposite situation, when the positrons propagate in the S-PB crystal (Fig. 3, *b*) first they run through the straight segment and then penetrate to the PB one. However, the positrons can channel in the straight segment with transverse energies higher than those in the PB segment. This leads to higher amplitudes of channeling oscillations in the straight segment. As a result, strong dechanneling occurs at the interface between the straight and the PB segments of the crystal (Note an increase in the dechanneling events in the region between 140 and 145 μm, see Fig. 3,*b*).

To illustrate the channeling properties of positrons, we plot the dependence of the primary fraction and the fraction of the channeled particles with account of re-channeling as functions of penetration distance z (Fig. 4). These dependencies can be used to analyze the intensities of the CUR and ChR peaks in the PB-S and S-PB crystals, since the intensity of radiation due to the periodic motion is proportional to the number of the particles participating in the quasi-periodic motion and to the square of the amplitude of corresponding oscillation [24, 25].

For 270 MeV positrons the dependencies of the primary fraction (see Fig. 4, *a*), and the fraction with account of re-channeling (Fig. 4,*b*) are almost identical for the both types of the crystals. In case of the S-PB crystal, the acceptance is higher than that for the PB-S one, due

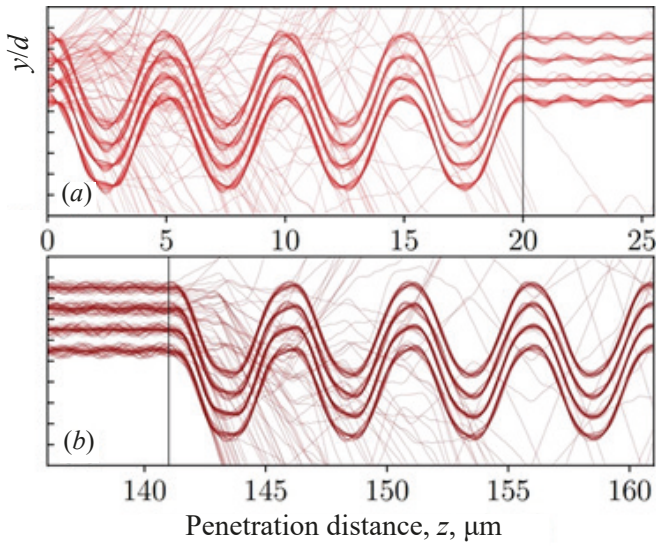

Fig. 3. Examples of 855 MeV positrons' trajectories (2D) propagating in the L_{cr} = 161 μm diamond PB-S (*a*) and S-PB (*b*) crystals; to highlight the processes which occur at the interfaces between PBC and SC the trajectories are zoomed into the windows with z = 0 − 25 μm (*a*) and 136 − 161 μm (*b*). The vertical black lines indicate the positions 20 μm (*a*) and 141 μm (*b*) of the interfaces between PB and the straight segments of the crystals

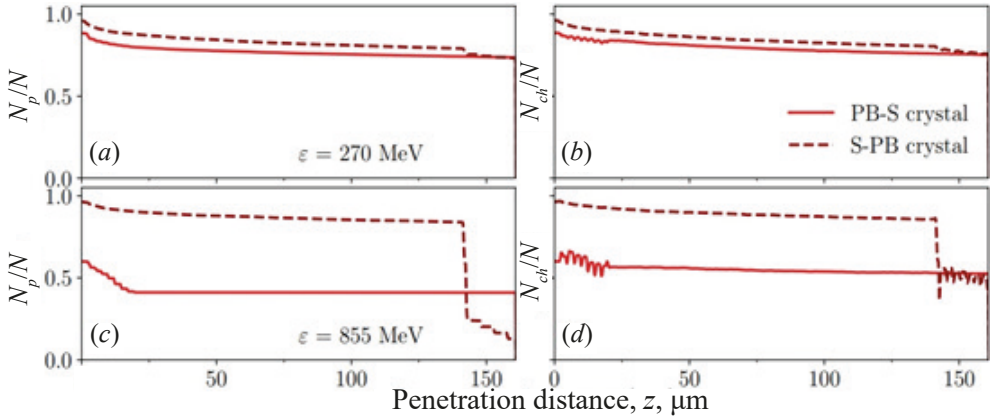

Fig. 4. Plots of the fractions of the channeling 270 MeV (*a*,*b*) and 855 MeV (*c*,*d*) positrons in the L_{cr} = 161 μm diamond (110) crystals vs their penetration distances; the primary fractions (*a*,*c*) and the fractions with account of the re-channeling (*b*,*d*) are presented

to the centrifugal force. Since the amplitudes of the periodic bending a are equal for the both types of crystals and the number of particles involved in the channeling motion in the PB parts of the crystals are approximately the same, the intensity of CUR should also be the same (see Fig. 2). This statement is true for the intensity of ChR. The centrifugal force is small and, as a result, a change in the channeling amplitudes is also small [24]. Thus, the number of channeled particles in the PB-S and the S-PB crystals are comparable.

For 855 MeV positrons the situation differs due to an increase in the centrifugal force in the PB parts of the crystals. The number of particles involved into the channeling motion drops as well as alternates the amplitude of channeling oscillations. The primary fraction of the positrons in the PB-S crystal steadily drops every time when the particles propagate through the segments of the crystal with a high curvature (note the step-like dependence at the first 20 μm in Fig. 4,*c*). However, in the straight segment of the crystal this dependence remains constant, since the centrifugal force caused by the crystal bending is absent in the straight segment of the crystal. Account for re-channeling gives rise to oscillations of the number of the channeled particles in the PB segment and the rise of the number of channeling particles in the straight segment.

In case of the S-PB crystal, the value of acceptance for 855 MeV positrons is higher and no significant re-channeling occurs in the straight part of the crystal. However, the drastic drop in the number of primary particles appears at the interface. This happens due to appearance of the centrifugal force in the PB part of the crystal. The number of channeling particles with account of re-channeling becomes approximately equal to that of particles in the channeling regime in case of the PB-S crystal (see Fig. 4,*d*). As a result of such behavior of the channeled positrons, the intensity of CUR is approximately the same. But the intensity of ChR for the PB-S crystal should be about 2 times smaller than that for the S-PB crystal (see Fig. 2,*b*).

To conclude, two main effects are observed for the positrons in the two types of crystals:

(*i*) For the two cases considered, the ChR intensities are the same within a margin of errors for ε = 270 MeV and differ at least two times for ε = 855 MeV positrons.

(*ii*) The ChR intensities are the same for the both types of crystals. This result can be explained by the presence of the centrifugal force in the PB segments of the crystal.

Results and discussion for electrons

Let us now return to the analysis of electron channeling in the heterocrystals. Electrons, in contrast to positrons, move around crystalline chains. This causes an increase in the number of hard collisions with bulk constituents and thus the dechanneling/re-channeling rates.

The anharmonicity of the interaction potential between ultra-relativistic electrons and lattice

atoms results in significant broadening of the peaks. The examples of the spectra are shown in Fig. 5.

In Fig. 5,*a* the results for 270 MeV electrons are presented. For the given electron energy, the intensities of ChR for the two geometries coincide within the margin of statistical error. For the PB-S crystal the small bump corresponding to the CUR arises in the radiation spectra around $\hbar\omega \approx 0.13$ MeV. In case of the S-PB crystal there is almost no peak.

For 855 MeV electrons the intensities of ChR differ by about one and a half times. The CUR for 855 MeV electrons in the PB-S crystal reveals itself as a peak at the photon energy $\hbar\omega \approx 0.7$ MeV. This peak is much more pronounced for 855 MeV electrons than that for 270 MeV ones, and it is almost absent for the S-PB crystal.

In order to understand these behaviors, one can plot the dependencies of a fraction of accepted electrons (Fig. 6,*a*,*c*) and a fraction of electrons with account of re-channeling (Fig. 6,*b*,*d*) upon the penetration distances. As for positrons, the value of N_p/N at $z = 0$ corresponds to the acceptance value. For the PB-S crystal the acceptance is determined by the PB part of it. Thus it is reduced by the presence of the centrifugal force. For the S-PB crystal the acceptance is the same as that in the straight crystal.

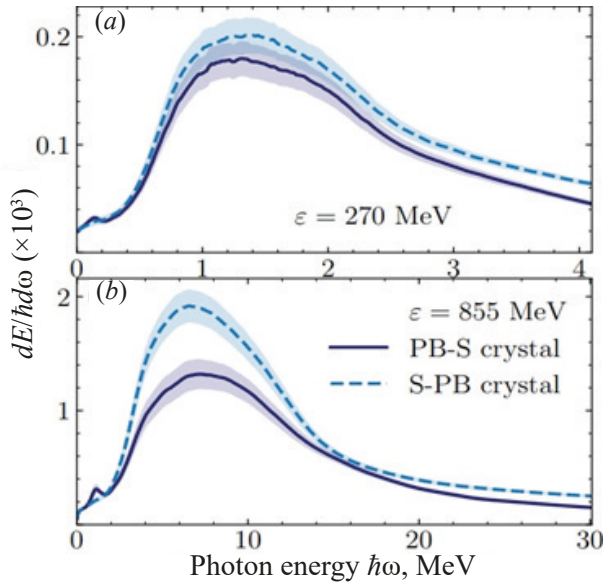

Fig. 5. The results for electrons similar to those shown in Fig. 2

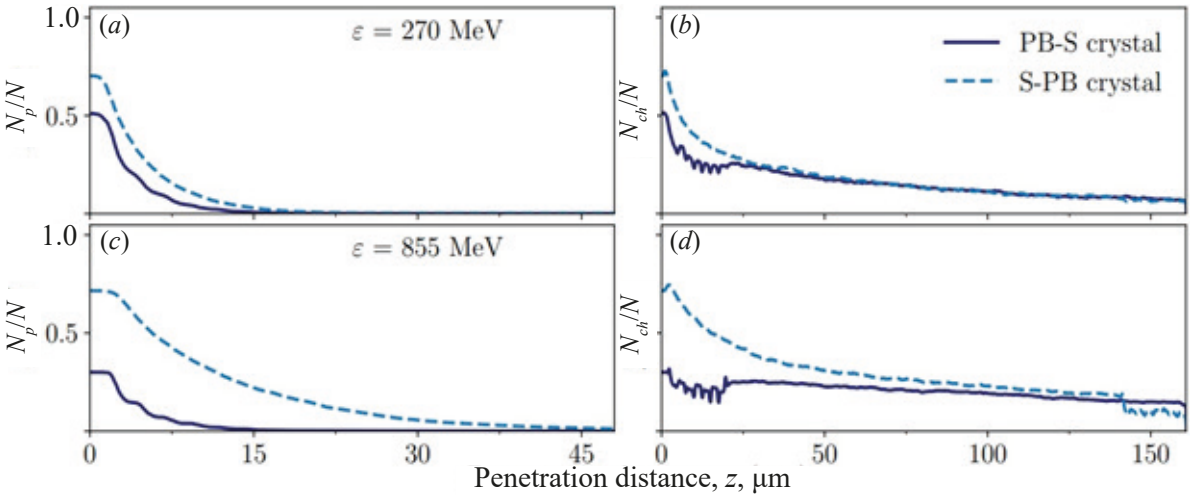

Fig. 6. The results for electrons similar to those shown in Fig. 4

Compared to positrons, electrons have significantly shorter dechanneling lengths, this leads to the fact that the number of the primary fraction of channeled electrons practically dies out for the crystal thicknesses over 50 μm, both for the PB-S and the S-PB crystals. At both energies of 270 and 855 MeV CUR forces a particle to pass at least one full channel period of the CU. If the channeling length becomes shorter than a half of CU period, photon emission by electrons becomes similar to synchrotron radiation. Taking into account the dynamics of dechanneling/re-channeling of electrons in the PBC [26], the main contribution to CUR is produced by particles accepted into the channeling regime [24]. This explains why CUR arises in the spectra mostly in case of the PB-S crystal. Also, it explains why this peak is more pronounced for 855 MeV electrons than that for 270 MeV ones.

The ChR intensity is proportional to the number of the particles involved in channeling the motion. The difference in the number of channeled electrons with energy 270 MeV in these two cases (see Fig. 6,*b*) manifests itself only at the first 20 μm of the whole penetration distance inside the crystals. Beyond this region the difference is negligible. This results in a small difference in the ChR intensities for 270 MeV electrons (in the two cases considered), the difference falling within the margin of error. For ε = 855 MeV the difference in the number of the channeled electrons becomes significant, leading to a larger difference in the spectral ChR intensities in Fig. 5,*b*.

To conclude this section let us state:

1. For the two cases considered, the ChR intensities are the same within margin of errors for ε = 270 MeV and become different for the 855 MeV electrons.

2. The CUR intensity vanishes in case of the S-PB crystals and is present in case of the PB-S ones.

Such behavior, as for the positrons, can be explained by the centrifugal force acting on the electrons in the PB segments of the crystals. The manifestation of CUR is also determined by a relatively short dechanneling length of electrons with respect to positrons.

Conclusions

In summary, the channeling and radiation phenomena for 270 and 855 MeV positrons and electrons in the oriented diamond heterocrystals have been simulated by means of all-atom relativistic molecular dynamics. We predict the radiation spectra for the two orientations (PB-S and S-PB) of crystals with respect to the beam. In case of positrons the CUR peaks are clearly

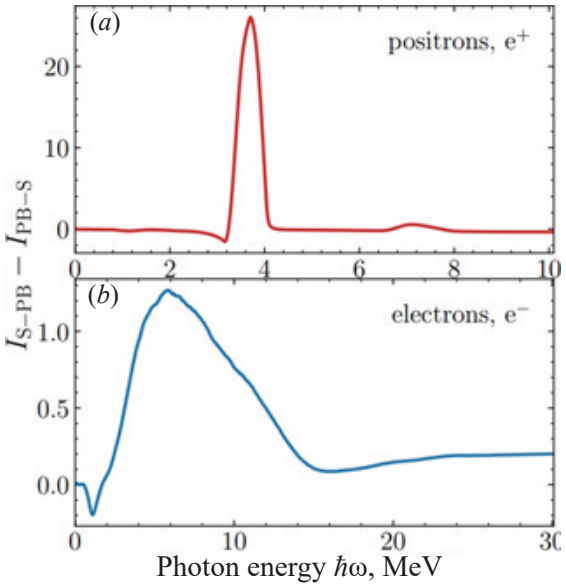

Fig. 7. The differences between radiation intensities for two propagation directions of positrons (*a*) and electrons (*b*) with 855 MeV energies vs photon ones. The data was taken from Figs. 2,*b* and 5,*b* respectively. $I_{S\text{-}PB}$ and $I_{PB\text{-}S}$ mean the radiation spectral densities $dE/\hbar d\omega$ for the particles propagating in the S-PB and PB-S crystals respectively

distinguishable from the background and have comparable intensity with respect to the ChR ones.

However, in case of electrons, the CUR peaks' observation over the broad ChR one becomes a challenging task, especially at low energies. This prediction opens a possibility for the experimental detection of the CUR peak in the PB structures grown on a substrate.

One possible way to analyze experimental data for such systems is to measure the radiation spectra for particles propagating in the PB-S and S-PB crystals and analyze their ratio. Such analysis is exemplified in Fig. 7. In this case not only the enhancement of radiation in the CUR desired region, but also the difference in channeling radiation intensities can be a fingerprint of the PB segment inside the crystal.

Finally, the analysis performed demonstrates that applying PBC with a straight substrate does not provide advantages for the CUR production. However, in the cases when a high-quality PB crystals can only be produced as segments of heterocrystals, practical realization of CUs based on such crystals with high quality positron beams is a feasible task. Electron beams can be used for probing the quality of PB segments of heterocrystals.

Acknowledgments

We acknowledge the Supercomputing Center of Peter the Great Saint-Petersburg Polytechnic University (SPbPU, Russia) for providing the opportunities to carry out large-scale simulations.

We are grateful to Hartmut Backe and Werner Lauth (University of Mainz, Germany) for useful discussions, to Rostislav Ryabov (SPbPU, Russia) for reading the manuscript carefully.

REFERENCES

1. **Ledingham K. W. D, Singhall R. P., McKenna P., Spencer I.,** Laser-induced nuclear physics and applications, Europhys. News. 33 (4) (2002) 120–124.

2. **Ledingham K. W. D, McKenna P., Singhall R. P.,** Applications for nuclear phenomena generated by ultra-intense lasers, Sci. 300 (5622) (2003) 1107–1111.

3. **Hajima R., Hayakawa T., Kikuzawa N., Minehara E.,** Proposal of nondestructive radionuclide assay using a high-flux gamma-ray source and nuclear resonance fluorescence, J. Nucl. Sci. Technol. 45 (5) (2008) 441–451.

4. **Weon B. M., Je J. H., Hwu Y., Margaritondo G.,** Decreased surface tension of water by hard-X-ray irradiation, Phys. Rev. Lett. 100 (21) (2008) 217403.

5. **Korol A. V., Solov'yov A. V.,** Crystal-based intensive gamma-ray light sources, Eur. Phys. J. D. 74 (10) (2020) 1–17.

6. **Lindhard J.,** Influence of crystal lattice on motion of energetic charged particles, Kongel. Dan. Vidensk. Selsk., Mat.-Fys. Medd. 34 (14) (1965) 1–64.

7. **Korol A. V., Solov'yov A. V., Greiner W.,** Coherent radiation of an ultra-relativistic charged particle channelled in a periodically bent crystal, J. Phys. G: Nucl. Part. Phys. 24 (5) (1998) L45.

8. **Korol A. V., Solov'yov A. V., Greiner W.,** Photon emission by an ultrarelativistic particle channeling in a periodically bent crystal, Int. J. Mod. Phys. E. 81 (1) (1999) 49–100.

9. **Korol A. V., Solov'yov A. V., Greiner W.,** Channeling and radiation in periodically bent crystals, 2nd Ed., Springer Verlag, Berlin, Heildeberg, 2014.

10. **Mikkelsen U., Uggerhøj E.,** A crystalline undulator based on graded composition strained layers in a superlattice, Nucl. Instrum. Methods Phys. Res. B. 160 (3) (2000) 435–439.

11. **Backe H., Krambrich D., Lauth W., et al.,** Channeling and radiation of electrons in silicon single crystals and $Si_{1-x}Ge_x$ crystalline undulators, J. Phys.: Conf. Ser. 438 (1) (2013) 012017.

12. **Wistisen T. N., Andersen K. K., Yilmaz S., et al.,** Experimental realization of a new type of crystalline undulator, Phys. Rev. Lett. 112 (25) (2014) 254801.

13. **Wienands U., Gessner S., Hogan M. J., et al.,** Channeling and radiation experiments at SLAC, Nucl. Instrum. Methods Phys. Res. B. 402 (1 July) (2017) 11–15.

14. **Tran Thi T. N., Morse J., Caliste D., et al.,** Synchrotron Bragg diffraction imaging characterization of synthetic diamond crystals for optical and electronic power device applications, J. Appl. Cryst. 50 (2) (2017) 561–569.

15. **De la Mata Guzman B., Sanz-Hervas A., Dowsett M. G., et al.,** Calibration of boron concentration in CVD single crystal diamond combining ultralow energy secondary ions mass

spectrometry and high resolution X-ray diffraction, Diamond and Related Materials. 16 (4–7) (2007) 809–814.

16. **Uggerhøj U. I.,** The interaction of relativistic particles with strong crystalline fields, Rev. Mod. Phys. 77 (4) (2005) 1131.

17. **Boshoff D., Copeland M., Haffejee F., et al.,** The search for diamond crystal undulator radiation, Proc. the 6-th Ann. Conf. of the South African Institute of Phys. (SAIP-2016), Johannesburg, South Africa, July 4–8 (2016) 112–117.

18. **Backe H., Lauth W.,** Channeling experiments with electrons at the Mainz Microtron {MAMI}, In: The 4th Int. Conf. "Dynamics of Systems on the Nanoscale", Oct. 3–7, 2016, Bad Ems, Germany, Book of Abstracts (2016) 58–58.

19. **Backe H., Lauth W., Tran Thi T. N.,** Channeling experiments at planar diamond and silicon single crystals with electrons from the Mainz Microtron {MAMI}, J. Instrum. 13 (04) (2018) C04022.

20. **Backe H., Krambrich D., Lauth W., et al.,** Future aspects of {X}-ray emission from crystal undulators at channeling of positrons, Nuovo Cimento. C. 34 (4) (2011) 175–180.

21. **Solov'yov I. A., Yakubovich A. V., Nikolaev P. V., et al.,** MesoBioNano explorer – A universal program for multiscale computer simulations of complex molecular structure and dynamics, J. Comput. Chem. 33 (30) (2012) 2412–2439.

22. **Sushko G. B., Bezchastnov V. G., Solov'yov I. A., et al.,** Simulation of ultra-relativistic electrons and positrons channeling in crystals with MBN Explorer, J. Comput. Phys. 252 (1 November) (2013) 404–418.

23. **Shen H., Zhao Q., Zhang F. S., et al.,** Channeling and radiation of 855 MeV electrons and positrons in straight and bent tungsten (110) crystals, Nucl. Instrum. Methods Phys. Res. B. 424 (1 June) (2018) 26–36.

24. **Pavlov A. V., Korol A. V., Ivanov V. K., Solov'yov A. V.,** Interplay and specific features of radiation mechanisms of electrons and positrons in crystalline undulators, J. Phys. B: At., Mol. Opt. Phys. 52 (11) (2019) 11LT01.

25. **Pavlov A. V., Korol A. V., Ivanov V. K., Solov'yov A. V.,** Channeling of electrons and positrons in straight and periodically bent diamond (110) crystals, Eur. Phys. J. D. 74 (2) (2020) 21.

26. **Korol A. V., Bezchastnov V. G., Solov'yov A. V.,** Channeling and radiation of the 855 MeV electrons enhanced by the re-channeling in a periodically bent diamond crystal, Eur. Phys. J. D. 71 (6) (2017) 174.

27. **Baier V. N., Katkov V. M., Strakhovenko V. M.,** Electromagnetic processes at high energies in oriented single crystals, World Scientific, Singapore, 1998.

СПИСОК ЛИТЕРАТУРЫ

1. **Ledingham K. W. D, Singhall R. P., McKenna P., Spencer I.** Laser-induced nuclear physics and applications // Europhysics News. 2002. Vol. 33. No. 4. Pp. 120–124.

2. **Ledingham K. W. D., McKenna P., Singhall R. P.** Applications for nuclear phenomena generated by ultra-intense lasers // Science. 2003. Vol. 300. No. 5622. Pp. 1107–1111.

3. **Hajima R., Hayakawa T., Kikuzawa N., Minehara E.** Proposal of nondestructive radionuclide assay using a high-flux gamma-ray source and nuclear resonance fluorescence // Journal of Nuclear Science and Technology. 2008. Vol. 45. No. 5. Pp. 441–451.

4. **Weon B. M., Je J. H., Hwu Y., Margaritondo G.** Decreased surface tension of water by hard-X-ray irradiation // Physical Review Letters. 2008. Vol. 100. No. 21. P. 217403.

5. **Korol A. V., Solov'yov A. V.** Crystal-based intensive gamma-ray light sources // The European Physical Journal D. 2020. Vol. 74. No. 10. Pp. 1–17.

6. **Lindhard J.** Influence of crystal lattice on motion of energetic charged particles // Kongelige Danske Videnskabernes Selskab, Matematisk-Fysiske Meddelelser. 1965. Vol. 34. No. 14. Pp. 1– 64.

7. **Korol A. V., Solov'yov A. V., Greiner W.** Coherent radiation of an ultrarelativistic charged particle channelled in a periodically bent crystal // Journal of Physics. G: Nuclear and Particle Physics. 1998. Vol. 24. No. 5. P. L45.

8. **Korol A. V., Solov'yov A. V., Greiner W.** Photon emission by an ultrarelativistic particle channeling in a periodically bent crystal // International Journal of Modern Physics. E. 1999. Vol. 81. No. 1. Pp. 49–100.

9. **Korol A. V., Solov'yov A. V., Greiner W.** Channeling and radiation in periodically bent crystals.

2nd edition. Berlin, Heildeberg: Springer Verlag, 2014. 240 p.

10. **Mikkelsen U., Uggerhøj E.** A crystalline undulator based on graded composition strained layers in a superlattice // Nuclear Instruments and Methods in Physics Research. B. 2000. Vol. 160. No. 3. Pp. 435–439.

11. **Backe H., Krambrich D., Lauth W., Andersen K. K., Hansen J. L., Uggerhøj U. I.** Channeling and radiation of electrons in silicon single crystals and $Si_{1-x}Ge_x$ crystalline undulators // Journal of Physics: Conference Series. 2013. Vol. 438. No. 1. P. 012017.

12. **Wistisen T. N., Andersen K. K., Yilmaz S., Mikkelsen R., Hansen J. L., Uggerhøj U. I., Lauth W., Backe H.** Experimental realization of a new type of crystalline undulator // Physical Review Letters. 2014. Vol. 112. No. 25. P. 254801.

13. **Wienands U., Gessner S., Hogan M. J., et al.** Channeling and radiation experiments at SLAC // Nuclear Instruments and Methods in Physics Research. B. 2017. Vol. 402. 1 July. Pp. 11–15.

14. **Tran Thi T. N., Morse J., Caliste D., et al.** Synchrotron Bragg diffraction imaging characterization of synthetic diamond crystals for optical and electronic power device applications // Journal of Applied Crystallography. 2017. Vol. 50. No. 2. Pp. 561–569.

15. **De la Mata Guzman B., Sanz-Hervas A., Dowsett M. G., Schwitters M., Twitchen D.** Calibration of boron concentration in CVD single crystal diamond combining ultralow energy secondary ions mass spectrometry and high resolution X-ray diffraction // Diamond and Related Materials. 2007. Vol. 16. No. 4–7. Pp. 809–814.

16. **Uggerhøj U. I.** The interaction of relativistic particles with strong crystalline fields // Reviews of Modern Physics. 2005. Vol. 77. No. 4. P. 1131.

17. **Boshoff D., Copeland M., Haffejee F., et al.** The search for diamond crystal undulator radiation // Proceedings of the 6-th Annual Conference of the South African Institute of Physics (SAIP-2016), Johannesburg, South Africa, July 4–8, 2016. Pp. 112–117.

18. **Backe H., Lauth W.** Channeling experiments with electrons at the Mainz Microtron {MAMI} // The 4th International Conference "Dynamics of Systems on the Nanoscale". Bad Ems, Germany, October 3–7, 2016. Book of Abstracts, 2016. Pp. 58–58.

19. **Backe H., Lauth W., Tran Thi T. N.** Channeling experiments at planar diamond and silicon single crystals with electrons from the Mainz Microtron {MAMI} // Journal of Instrumentation. 2018. Vol. 13. No. 04. P. C04022.

20. **Backe H., Krambrich D., Lauth W., et al.** Future aspects of {X}-ray emission from crystal undulators at channeling of positrons// Il Nuovo Cimento. C. 2011. Vol. 34. No. 4. Pp. 175–180.

21. **Solov'yov I. A., Yakubovich A. V., Nikolaev P. V., Volkovets I., Solov'yov A. V.** MesoBioNano explorer – A universal program for multiscale computer simulations of complex molecular structure and dynamics // Journal of Computational Chemistry. 2012. Vol. 33. No. 30. Pp. 2412–2439.

22. **Sushko G. B., Bezchastnov V. G., Solov'yov I. A., Korol A. V., Greiner W., Solov'yov A. V.** Simulation of ultra-relativistic electrons and positrons channeling in crystals with MBN Explorer // Journal of Computational Physics. 2013. Vol. 252. 1 November. Pp. 404–418.

23. **Shen H., Zhao Q., Zhang F. S., Sushko G. B., Korol A. V., Solov'yov A. V.** Channeling and radiation of 855 MeV electrons and positrons in straight and bent tungsten (110) crystals // Nuclear Instruments and Methods in Physical Research. B. 2018. Vol. 424. 1 June. Pp. 26–36.

24. **Pavlov A. V., Korol A. V., Ivanov V. K., Solov'yov A. V.** Interplay and specific features of radiation mechanisms of electrons and positrons in crystalline undulators // Journal of Physics B: Atomic, Molecular and Optical Physics. 2019. Vol. 52. No. 11. P. 11LT01.

25. **Pavlov A. V., Korol A. V., Ivanov V. K., Solov'yov A. V.** Channeling of electrons and positrons in straight and periodically bent diamond (110) crystals // The European Physical Journal. D. 2020. Vol. 74. No. 2. P. 21.

26. **Korol A. V., Bezchastnov V. G., Solov'yov A. V.** Channeling and radiation of the 855 MeV electrons enhanced by the re-channeling in a periodically bent diamond crystal // The European Physical Journal. D. 2017. Vol. 71. No. 6. P. 174.

27. **Байер В. Н., Катков В. М., Страховенко В. М.** Электромагнитные процессы при высокой энергии в ориентированных монокристаллах. Новосибирск: «Наука». Сибирское отделение, 1989. 400 с.

THE AUTHORS

PAVLOV Alexander V.
Peter the Great St. Petersburg Polytechnic University
29 Politechnicheskaya St., St. Petersburg, 195251, Russia
a.pavlov@physics.spbstu.ru

KOROL Andrei V.
MBN Research Center UG
3 Altenhoferallee, Frankfurt am Main, 60438, Germany
korol@mbnexplorer.com

IVANOV Vadim K.
Peter the Great St. Petersburg Polytechnic University
29 Politechnicheskaya St., St. Petersburg, 195251, Russia
ivanov@physics.spbstu.ru
ORCID: 0000-0002-3584-4583

SOLOV'YOV Andrey V.
MBN Research Center UG
3 Altenhoferallee, Frankfurt am Main, 60438, Germany
solovyov@mbnresearch.com
ORCID: 0000-0003-1602-6144

СВЕДЕНИЯ ОБ АВТОРАХ

ПАВЛОВ Александр Валерьевич – *аспирант кафедры физики Санкт-Петербургского политехнического университета Петра Великого, Санкт-Петербург, Россия.*
195251, Россия, г. Санкт-Петербург, Политехническая ул., 29
a.pavlov@physics.spbstu.ru

КОРОЛЬ Андрей Владимирович – *кандидат физико-математических наук, доцент, научный сотрудник Научно-исследовательского центра мезобионаносистем (MBN), г. Франкфурт-на-Майне, Германия.*
3, Altenhoferallee, Frankfurt am Main, 60438, Germany
korol@mbnexplorer.com

ИВАНОВ Вадим Константинович – *доктор физико-математических наук, профессор кафедры физики Санкт-Петербургского политехнического университета Петра Великого, Санкт-Петербурге, Россия.*
195251, Россия, г. Санкт-Петербург, Политехническая ул., 29
ivanov@physics.spbstu.ru
ORCID: 0000-0002-3584-4583

СОЛОВЬЕВ Андрей Владимирович – *доктор физико-математических наук, ведущий научный сотрудник Научно-исследовательского центра мезобионаносистем (MBN), г. Франкфурт-на-Майне, Германия.*
3, Altenhoferallee, Frankfurt am Main, 60438, Germany
solovyov@mbnresearch.com
ORCID: 0000-0003-1602-6144

Received 11.10.2021. Approved after reviewing 18.10.2021. Accepted 18.10.2021.
Статья поступила в редакцию 11.10.2021. Одобрена после рецензирования 18.10.2021. Принята 18.10.2021.